

2004

# Coherent and noncoherent receivers for asymmetric modulation

Eric Eugene Kreb  
*San Jose State University*

Follow this and additional works at: [https://scholarworks.sjsu.edu/etd\\_theses](https://scholarworks.sjsu.edu/etd_theses)

---

## Recommended Citation

Kreb, Eric Eugene, "Coherent and noncoherent receivers for asymmetric modulation" (2004). *Master's Theses*. 2638.  
DOI: <https://doi.org/10.31979/etd.sr7h-mysg>  
[https://scholarworks.sjsu.edu/etd\\_theses/2638](https://scholarworks.sjsu.edu/etd_theses/2638)

This Thesis is brought to you for free and open access by the Master's Theses and Graduate Research at SJSU ScholarWorks. It has been accepted for inclusion in Master's Theses by an authorized administrator of SJSU ScholarWorks. For more information, please contact [scholarworks@sjsu.edu](mailto:scholarworks@sjsu.edu).

COHERENT AND NONCOHERENT RECEIVERS  
FOR  
ASYMMETRIC MODULATION

A Thesis

Presented to

The Faculty of the Department of  
Electrical Engineering

San Jose State University

In Partial Fulfillment

Of the Requirements for the Degree  
Master of Electrical Engineering

By

Eric Eugene Krebs

August 2004

UMI Number: 1424509

Copyright 2004 by  
Kreb, Eric Eugene

All rights reserved.

### INFORMATION TO USERS

The quality of this reproduction is dependent upon the quality of the copy submitted. Broken or indistinct print, colored or poor quality illustrations and photographs, print bleed-through, substandard margins, and improper alignment can adversely affect reproduction.

In the unlikely event that the author did not send a complete manuscript and there are missing pages, these will be noted. Also, if unauthorized copyright material had to be removed, a note will indicate the deletion.

**UMI**<sup>®</sup>

---

UMI Microform 1424509

Copyright 2005 by ProQuest Information and Learning Company.

All rights reserved. This microform edition is protected against  
unauthorized copying under Title 17, United States Code.

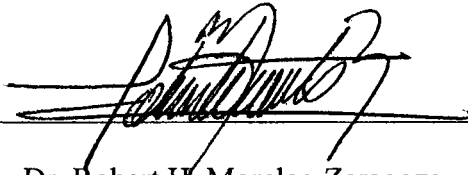
ProQuest Information and Learning Company  
300 North Zeeb Road  
P.O. Box 1346  
Ann Arbor, MI 48106-1346

© 2004

Eric Eugene Kreb

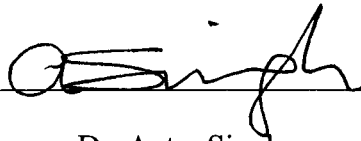
ALL RIGHTS RESERVED

Approved for the Department of Electrical Engineering



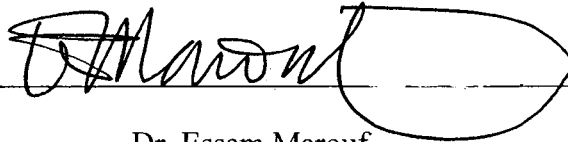
A handwritten signature in black ink, appearing to read 'R. Morelos-Zaragoza', written over a horizontal line.

Dr. Robert H. Morelos-Zaragoza



A handwritten signature in black ink, appearing to read 'A. Singh', written over a horizontal line.

Dr. Avtar Singh



A handwritten signature in black ink, appearing to read 'E. Marouf', written over a horizontal line.

Dr. Essam Marouf

Approved for the University



A handwritten signature in black ink, appearing to read 'Paul C. Stok', written over a horizontal line.

## ABSTRACT

### COHERENT AND NONCOHERENT RECEIVERS

FOR

### ASYMMETRIC MODULATION

By Eric Eugene Krebs

This thesis presents asymmetric modulation schemes for fully adaptable signal designs that open new opportunities for error reduction in noise induced channels. Two categories of design are addressed, asymmetric phase-shift keying and asymmetric quadrature-amplitude modulation. The former is a continuously modified phase-shift keying signal; the latter a discretely selective quadrature-amplitude modulation signal that offers several constellations based on optimal lattice structure design, which can also be continuously modified similar to the asymmetric phase-shift keying design. Performance analysis is presented for these constellations in added white Gaussian noise for coherent and noncoherent reception using MATLAB, and arguments are presented for improved constellation design and synchronization. Asymmetric coherence, optimal density constellation design, dynamically controlled signaling schemes, and a general algorithm for generating quasi-Gray codes are presented as original contributions in this study.

## ACKNOWLEDGMENT

I would like to express my gratitude to Dr. Robert Morelos-Zaragoza for his continued inspiration and guidance throughout the making of this thesis, as well as for his patience in the proofreading of the text. His helpful and generous advice and suggestions have greatly improved my work. I would also like to thank Dr. Essam Marouf and Dr. Avtar Singh for their careful reading of the complete version of this paper, and for their critical analysis and suggestions for further development of the ideas presented.

## TABLE OF CONTENTS

	Page
List of Figures	viii-iv
1. Introduction	1
2. Communication Systems Theory	6
2.1 Transmitter	
2.2 Channel	
2.2.1 Noise	
2.2.2 Fading	
2.2.3 Phase Error	
2.3 Receiver	
2.3.1 Synchronization	
2.3.2 Data-Aided Synchronization	
2.3.3 Noncoherent Receivers	
2.4 Complex Baseband System Model	
3. Modulation Theory	15
3.1 Orthogonal Base Functions	
3.2 Power Minimization	
3.3 Nearest Neighbor Significance	
3.4 Constellation Lattice	
3.4 Gray Coding	



3.5	Analysis	
4.	Asymmetric Constellation Design	31
4.1	Early Approaches	
4.2	Asymmetric Phase-Shift Keying	
4.3	Asymmetric Quadrature-Amplitude Modulation	
4.4	Characteristics Benefits of Asymmetric Modulation	
5.	Asymmetric Receivers	42
5.1	Coherent Receivers	
5.2	Noncoherent Receivers	
6.	Future Research	49
7.	Conclusion	50
	References	51

## LIST OF FIGURES

	Page
Figure 2.1 Digital Communication System	6
Figure 2.2 Fading Channel Manifestations	9
Figure 2.3 Difference between Additive Noise and Phase Error	10
Figure 2.4 8-PSK & 16-QAM: Signal Space Vector Diagram	11
Figure 2.5 Coherent and Noncoherent Receivers	13
Figure 2.6 Complex Baseband System	14
Figure 3.1 $N$ Orthonormal Basis Functions	16
Figure 3.2 Bandpass Modulation	16
Figure 3.3 Lattice Structures	19
Figure 3.4 Nearest Neighbor Distance Analysis of Lattice Structures	19
Figure 3.5 Significance of Next-to-Nearest Neighbor Intersymbol Distances	20
Figure 3.6 Maximizing Euclidian Distance for Large Hamming Distances	21
Figure 3.7 Common Gray Code for Standard 16-QAM	23
Figure 3.8 Probability of Error between Two Symbols in AWGN	27
Figure 3.9 Two Dimensional Integration Region for Gaussian PDF	28
Figure 3.10 Comparison of Union Bound and Theoretical Analysis	30
Figure 4.1 Initial Study into Phase-Invariant Modulation	32
Figure 4.2 AsPSK Mapping Functions	33
Figure 4.3 AsPSK Constellations	34
Figure 4.4 AsPSK for Various $\alpha_1$ parameters	34

Figure 4.5	AsPSK for Various $\alpha_2$ parameters	35
Figure 4.6	AsQAM-v1, $\beta=[1, 2, 3, 4]$	37
Figure 4.7	AsQAM-v2, $\beta=[1, 2, 3, 4]$	38
Figure 4.8	Signal Space Vector Diagrams for Symmetric and Asymmetric Signals	39
Figure 5.1	Precise Performance Control of AsPSK, against PSK & DPSK	43
Figure 5.2	Diverse Performance Control of AsPSK, against PSK & DPSK	44
Figure 5.3	Performance Advantage of AsQAM over QAM	45
Figure 5.4	Asymmetrically Coherent Receiver	46
Figure 5.5	Simulation of Asymmetric Coherent Receiver with AsPSK-v1	48
Figure 5.6	Simulation of Asymmetric Coherent Receiver with AsPSK-v2	48

## 1. INTRODUCTION

The basic system model for digital commutation is composed of a transmitter that sends source information into a channel and a receiver that attempts to recover the original data on the opposite side of the channel. The two primary communication resources are transmit power, the average power of the transmitted signal, and channel bandwidth, the band of frequencies allocated for the transmission of the message signal. Depending on the communication channel, one of these resources are typically more critical than the other; therefore, channels are often classified as “power limited” or “band limited.” To conserve these resources, modulation schemes are developed to minimize their costs.

A basic modulation scheme for transmitting the data is pulse-amplitude modulation (PAM), which uses quantized signal levels for sequential transmission of information. To limit the bandwidth of PAM signals, a transmit filter is applied to the baseband signal before modulating the center frequency to a desired value; a common transmit filter is produced with the raised cosine pulse [1]. Further improvement is achieved by modulating these PAM signals along two or more orthogonal channels to form basis functions in N-dimensional signal space, constructing multi-dimensional constellations.

These signaling schemes can be classified into constant envelope and modulated envelope signals: constant envelope signals have equal energy among symbols within its representative constellation; modulated envelope signals have symbol energies that are

not all equal. The trade-offs of power efficiency, spectral efficiency, and device cost, lead to the choice of which modulation class to choose. Constant envelope signals are less power efficient than modulated envelope signals and can be implemented with non-linear amplifiers, which are less expensive devices than their linear counterparts. On the other hand, modulated envelope signals are spectrally efficient, implemented with linear amplifiers at higher device cost. These tradeoffs between channel types inspire the use of two common modulation designs, phase-shift keying (PSK) and quadrature-amplitude modulation (QAM).

Synchronization circuits have a nominal impact on the overall cost of receivers, so the search for more efficient synchronization models continues to be an ongoing research topic for design engineers [2]. This thesis will explain how the added reference parameters offered by asymmetric modulation can be used to facilitate lower cost and better performing devices for some or all of a receiver's synchronization needs: clock synchronization, phase synchronization, block synchronization.

Since standard PSK and QAM signaling schemes are geometrically symmetric, they lend themselves to the problem of phase ambiguity at the receiver. When the local oscillator at the receiver is synchronized to the transmit oscillator, phase ambiguity is solved, but there is a cost for this synchronization. Often a pilot signal is used or additional bits in the error correction code are used for synchronization; in either case bandwidth is spent for synchronization. When phase has been synchronized, the receiver is defined as coherent; while a receiver that does not require a priori knowledge of the phase is defined as noncoherent. Examples of noncoherent receivers that are not

corrupted by the phase ambiguity problem are the differentially coherent, differential phase-shift keying (DPSK) and differential quadrature-amplitude modulation (DQAM). Although the presented asymmetrically coherent receiver designed in this project does not improve upon the differentially coherent receiver, this thesis establishes asymmetric coherence with minimal signal-to-noise ratio (SNR) gain over DPSK, and in so, offers an alternative noncoherent design. Within the noncoherent design, this thesis, also, initiates efforts to exploit an error correction property inherent to asymmetric constellations.

An additive white Gaussian noise (AWGN) channel is a good model for the noise induced by the physical characteristics of the overall system, and the performance in this channel serves as a valid method for comparing different modulation schemes. The key to achieving optimal performance from signaling is in maximization of the nearest neighbor distances between symbols of the signal constellations; next-to-nearest neighbor distances will have less significant affects on modulation performance, yet these distances have nominal impact on the results and must be considered for the optimal design. Current PSK designs attempt optimal nearest neighbor distances by evenly spacing the symbols around the unit circle; current QAM designs relax the nearest neighbor rule to support an even number of symbols with symmetric constellations. Based on maximizing nearest neighbor distances within a constellation, this thesis will present an optimal lattice structure for QAM design and use MATLAB to simulate its performance in an AWGN channel and directly compare it to standard QAM.

Maximizing the nearest neighbor distances among symbols will minimize the signal error rate; however, minimizing bit error rate is the ultimate goal in digital

communication systems. Gray coding accomplishes this task, but as it is easy to Gray code for PSK and standard QAM, it becomes an impossible task for many QAM constellations that are not constructed of a square-lattice structure, where the best we can hope for is quasi-Gray coding. Asymmetric constellation alter the task of Gray coding or approaching Gray coding because the increased density of the constellations make it increasingly difficult to define decision regions among bits. A general algorithm is presented in this thesis for quasi-Gray code that can be applied to the most dense asymmetric constellations, while maintaining valid results for the Gray coding of common PSK and QAM constellations.

Given the freedom from symmetry, an endless multitude of arrangements are available. For PSK, mapping symmetric constellations to asymmetry involves choosing a phase mapping function for symbols, which can include an asymmetry parameter in the function definition that allows functional control for the user. For QAM, a random or methodical method of construction can be the foundation of the constellation. In this thesis, an optimal QAM lattice is presented with four similar arrangements and offers an improved design algorithm that bends that lattice as needed for improved performance. Further, an asymmetric parameter can be used to stretch the constellation along base functions to, again, give the user continuous, dynamic, functional control.

This thesis began as an original approach to solve the problem of phase ambiguity without the use of additional signaling or data. Once the idea was developed similar research was discovered in both the areas of AsPSK [3] and AsQAM [4]; however, the ideas presented here are from a fresh perspective and are intended to argue the untapped

potential that is inherent in the general area of asymmetric modulation. Original ideas for synchronization, modulation design, dynamic constellation control, and a general algorithm for approaching Gray code are presented in this thesis, and the argument is made for an added reference parameter to modern modulation theory: asymmetry.



## 2. COMMUNICATION SYSTEMS THEORY

Through the course of this thesis, the digital communication system model of Figure 2.1 will be considered, and the reduced, complex baseband system model of Figure 2.6 will be used for simulations.

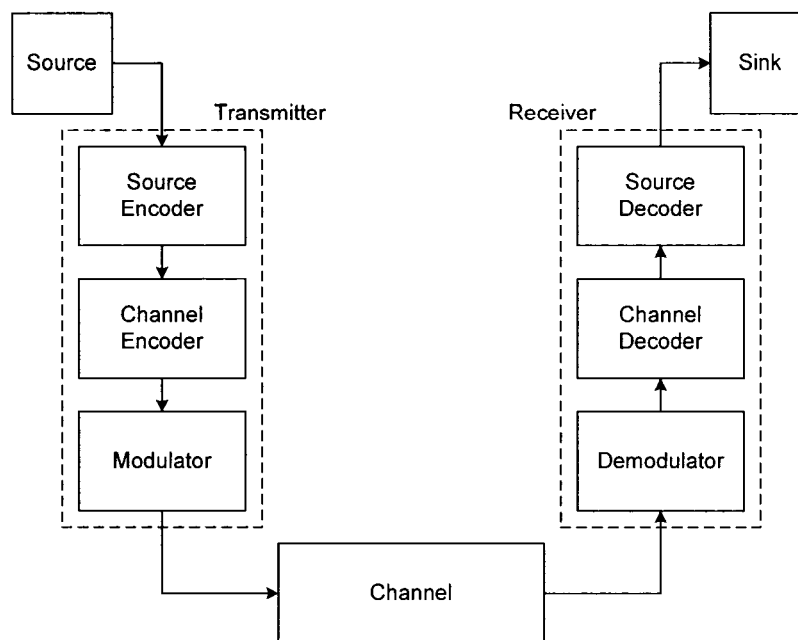


Figure 2.1 Digital Communication System

### 2.1 Transmitter

In the digital communication system model of Figure 2.1, the transmitter adapts the source signal to better use power and bandwidth, and compensate for impairments caused by the channel. Input to the transmitter, source information is in the form of an analog or digital signal that is digitally encoded by the source encoder, which removes redundant information to improve channel efficiency. The source encoder produces a

source code word that is processed by the channel encoder, which adds controlled redundancy to compensate for errors caused by the channel. Next, the channel encoder produces a channel code word that is then modulated to a waveform that is suitable for transmission over the channel. The modulator has the task of band-limiting the signal and translating that signal to a desired carrier frequency.

## 2.2 Channel

The channel is the link between transmitter and receiver that is modeled to include its own characteristics, as well as imperfections caused by the transmitter and receiver hardware.

### 2.2.1 Noise

The overall system noise is characterized by AWGN, which is an additive noise vector that is evenly distributed over the specified frequency band with the following Gaussian probability density function (PDF):

$$P_e(y) = \frac{1}{\sigma_y \sqrt{2\pi}} \exp\left(-\frac{(y - \mu_y)^2}{2\sigma_y^2}\right),$$

where  $y$  is a sample of the random variable  $Y$ ,  $\mu_y$  is the mean of  $Y$ , and  $\sigma_y$  is the standard deviation of  $Y$ . For reference later in this document, power spectral density of white noise is herein specified as  $N_0/2$ , leading to the autocorrelation function as the delta function weighted by the factor  $N_0/2$ .

### 2.2.2 Fading

The AWGN channel is modeled on the assumption that the received signal is affected only by constant attenuation and constant delay [5], [6]. Wireless channel models require an added complexity that is referred to as “fading,” which is the result of channel fluctuation, multi-path propagation, and relative movement between transmitter and receiver. Fading is manifested by reflection, diffraction, and scattering; the result are degradation affects that can be classified into two categories, large-scale and small-scale. Large-scale fading occurs over large distances and is due to prominent terrain contours such as mountains, trees, or clouds. Small-scale fading is due to small changes in the separation between transmitter and receiver and is manifested by time spreading of the signal and time variance of the channel. Small-scale, time-spread signals experience either frequency-selective fading, where time delays are greater than the signal period, or flat fading, where multi-path components arrive within the signal time duration. Small-scale, time-variant channels cause fast-fading, where the fading character of the channel will change several times during the time that a signal is propagating, and slow-fading, where the channel state can be expected to remain unchanged during the time that the signal is transmitted. An overview of fading issues is summarized in Figure 2.2.

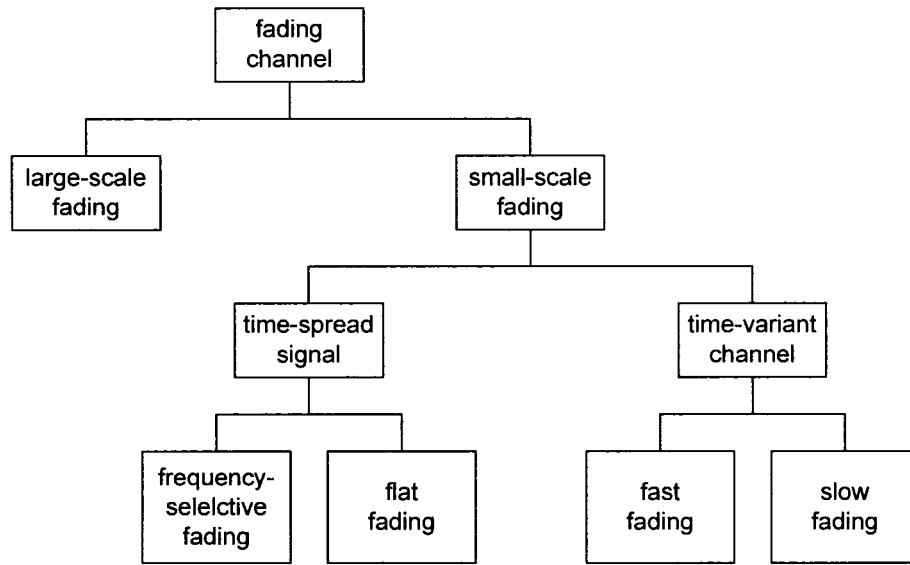


Figure 2.2 Fading Channel Manifestations

### 2.2.3 Phase Error

Another source of error to consider is phase estimation error, which is solved by the phase recovery circuit in the receiver. Inexact phase estimates for uncoded modulation can be modeled with a Gaussian PDF as follows:

$$P_e(\phi) = \frac{1}{\sigma_\phi \sqrt{2\pi}} \exp\left(-\frac{(\phi - \mu_\phi)^2}{2\sigma_\phi^2}\right),$$

with  $\phi$  as the rotational error of the complex plain [2]. Figure 2.3 graphically demonstrates the difference between AWGN and phase estimation error, in the complex plane.

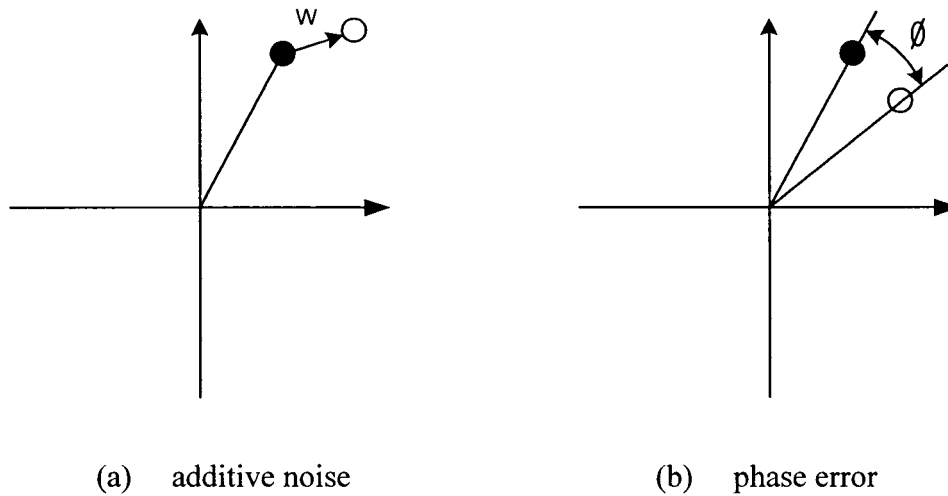


Figure 2.3 Difference between Additive Noise and Phase Error

### 2.3 Receiver

The receiver demodulates and decodes the channel output to recover the original information from the source. Once demodulated, the channel decoder, which is typically a filter matched to the channel encoder, is used to recover one sample estimate per symbol of the channel code word. The channel encoder estimates the digital source code word, which is then converted to an estimate of the original data by the source decoder. In the process, there are several synchronization issues.

#### 2.3.1 Synchronization

Synchronization can be classified into three major categories: timing synchronization, carrier synchronization, block synchronization. Timing synchronization refers to the ability of the receiver to sample at the optimal sampling rate. For a baseband PAM signal, the maximum eye opening in the eye diagram represents the optimal sample

positions. For baseband PSK and QAM, the extension of the eye diagram is presented in a signal space vector diagram; the greater openings represent optimal opportunities for timing. Examples for 8-PSK and 16-QAM signal space vector diagrams using a raised cosine filter, with rolloff factor of 0.6 and 0.95 respectfully, are presented in Figure 2.4. Carrier synchronization refers to the task of measuring correct frequency and phase. By definition, coherent receivers require a priori knowledge of signal phase, where noncoherent receivers do not. Block synchronization or frame synchronization are examples of the third synchronization class, where blocks of data are often encapsulated by a head and/or a tail for dynamic routing of multi-frame files or for error checking over a defined subset of bits transmitted in a data link. Block, or frame, synchronization generally require additional bits to the payload.

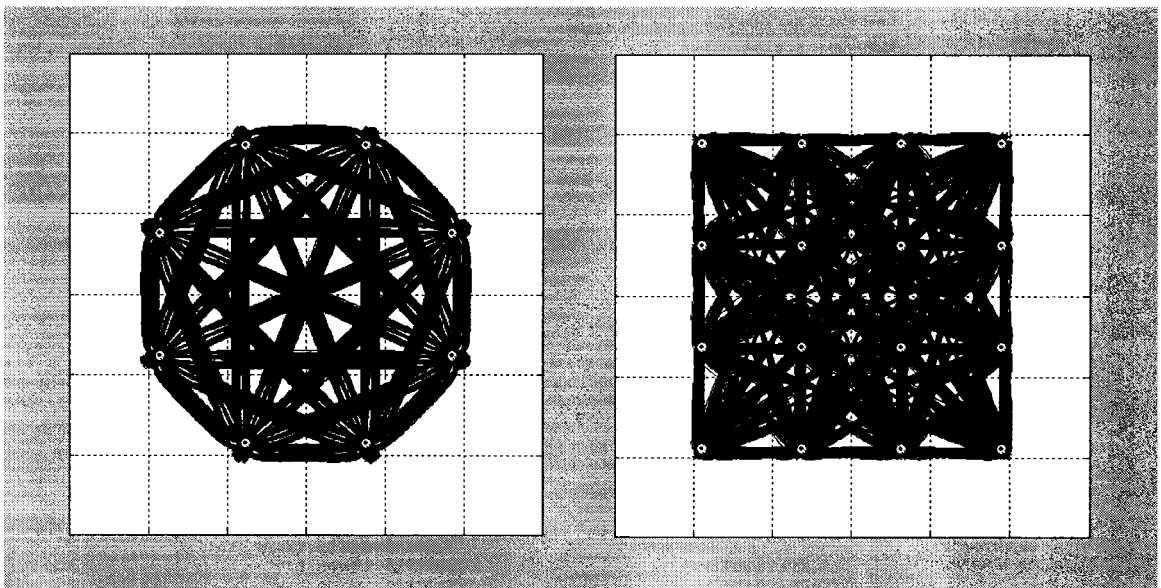


Figure 2.4 8-PSK & 16-QAM: Signal Space Vector Diagram

### 2.3.2 Data-Aided Synchronization

There are two fundamental implementations of phase synchronization to establish coherence: data-aided, nondata-aided. The former occupies extra bandwidth and transmit power; the later typically requires more time to establish synchronization [7].

### 2.3.3 Noncoherent Receivers

Noncoherent receivers need no provision for phase recovery. The advantage of noncoherent receivers is that they are simpler and more robust, but their error probability in the presence of noise is generally higher than for coherent receivers. An example of noncoherent receivers is the differentially coherent receiver. This paper will present the notion of the asymmetrically coherent receiver as another noncoherent alternative for reception. Block diagrams of coherent and noncoherent receivers are shown in Figure 2.5.

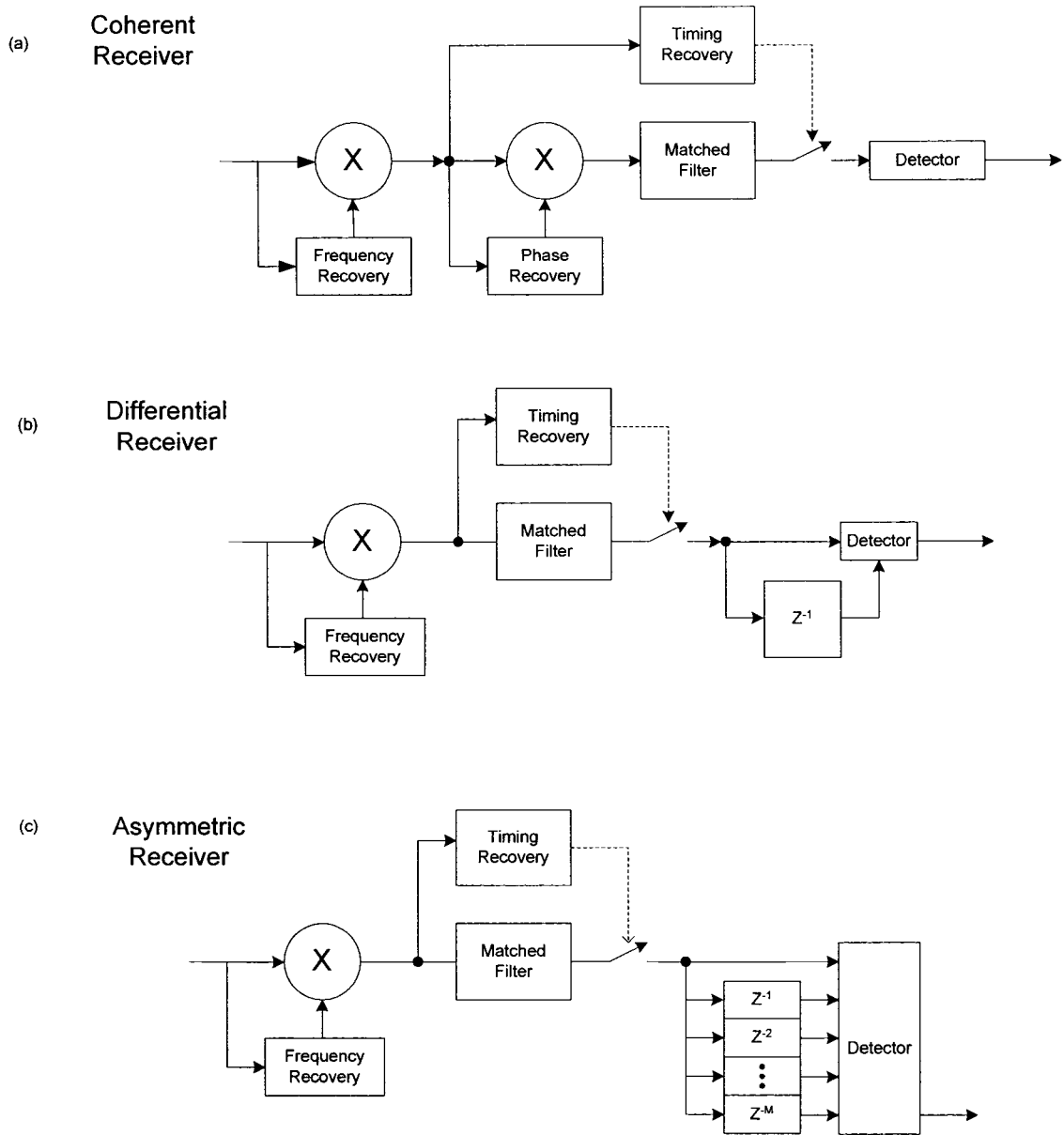


Figure 2.5 Coherent and Noncoherent Receivers

## 2.4 Complex Baseband System Model

The system model previously described can be reduced to minimize computational complexity in simulations and to focus on specific issues that will be



discussed. Baseband analysis can be used, since the carrier frequency does not influence the system and its performance. A wideband channel and perfectly matched ideal channel encoder and channel decoder will be assumed; in the case that matched filters are discussed, as in the signal space vector diagrams previously mentioned, root-raised cosine filters will be used. The resulting model is the “complex baseband system model,” where the channel takes a discrete complex signal and outputs a discrete complex signal that has been shifted due to the noise, fading, and phase error induced by the channel. For our discussion in this paper we will simulate the model with AWGN, and discuss the expectations of further research that will include fading and phase estimation error. The model for simulation is reduced to the representation in Figure 2.6.

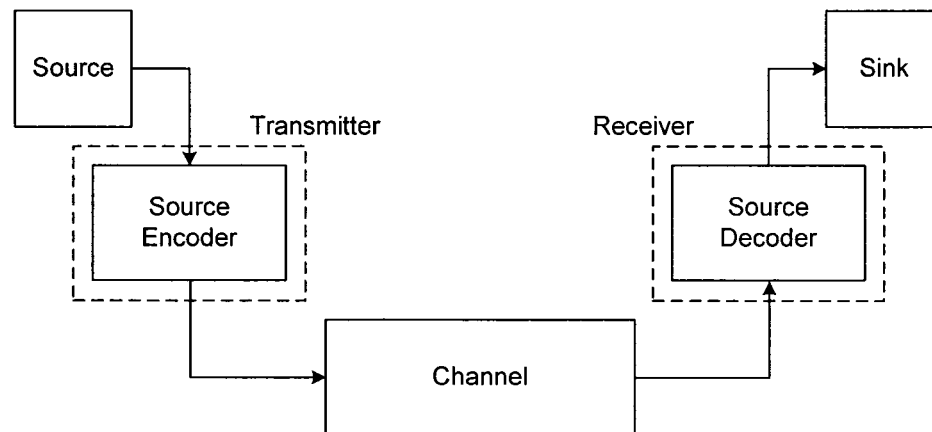


Figure 2.6 Complex Baseband System

### 3. MODULATION THEORY

Some fundamental concepts of modulation theory are visited in this chapter before attacking the actual designs of asymmetric modulation (AsM). It should be kept in mind that the primary modulation design goals include phase invariance and optimal performance in AWGN.

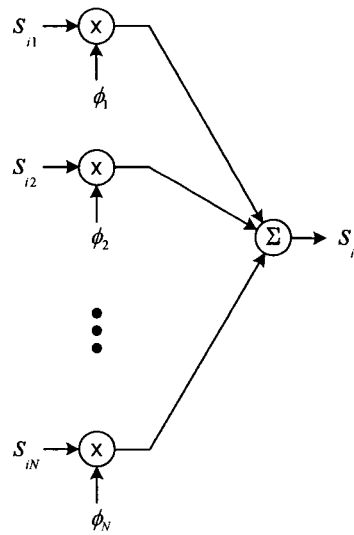
#### 3.1 Orthogonal Basis Functions

The constellations presented are extendable to  $N$  orthonormal basis functions, with each statistically independent basis function modulated by a PAM signal. Represented as a set of vectors in the complex and multi-dimensional realm, the full constellation will result in either constant envelope signals or modulated envelope signals. The vector of an  $N$ -dimensional constellation can be synthesized and analyzed by the structure represented in Figure 3.1, and although the asymmetric theory presented can be translated to  $N$  dimensions, the theory will be presented through design and simulation of the two dimensional bandpass scheme, shown in Figure 3.2, that maps components of two statistically independent basis functions, in-phase and quadrature, onto the complex plane such that each symbol can be represented by amplitude and phase [8]:

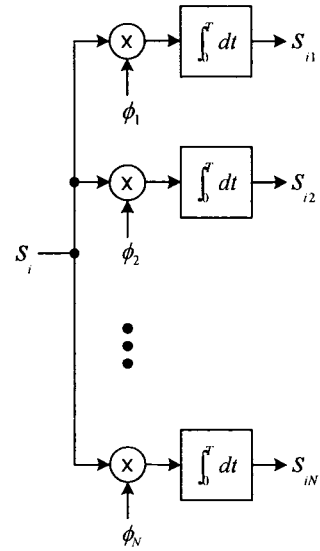
$$s(t) = s_I(t) \cos(2\pi f_c t) - s_Q(t) \sin(2\pi f_c t)$$

$$s = s_I + j \cdot s_Q$$

$$s = |s| e^{j\theta}$$

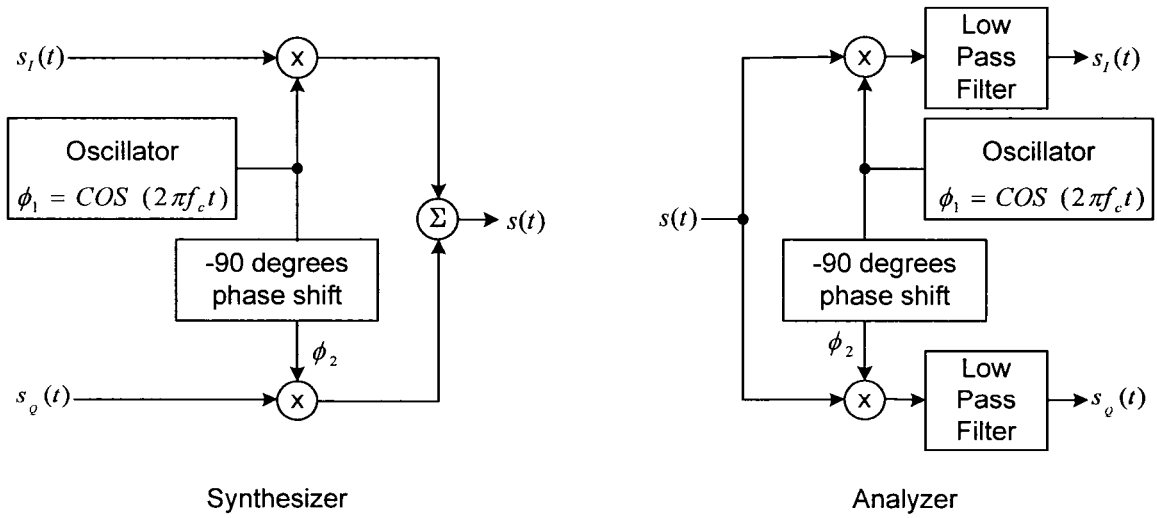


Synthesizer



Analyzer

Figure 3.1 *N* Orthonormal Basis Functions



Synthesizer

Analyzer

Figure 3.2 Bandpass Modulation

### 3.2 Power Minimization

In order to minimize the required transmit power, the average energy of potential symbols needs to be minimized in the AsQAM scheme. Moving the energy centroid of the constellation to the origin of the complex plane will result in minimum average symbol energy that will lead to greater normalized intersymbol distance and better performance in noisy environments.

Since AsPSK requires equal energy for all symbols, this method of power minimization does not apply. Furthermore, rotation of axis about the origin will not change the overall power, so once optimized, a given phase shift applied to all symbols would have no effect to power efficiency. For example, when a constant envelope is required for a 4-symbol constellation, a quadriphase-shift keying (QPSK) constellation is optimal, and has phases,

$$\theta = \left( \frac{1}{2} + k \right) \cdot \frac{\pi}{2}, \quad k=1,2,3,4,$$

so the equally optimal 4-PSK with phase

$$\theta = \frac{k \cdot \pi}{2}, \quad k=1,2,3,4,$$

results with equal efficiency.

### 3.3 Nearest Neighbor Significance

Given the AWGN channel, a stronger potential for error exists for nearest neighboring symbols within a constellation. There is a decreasing precedence order for increasing nearest neighbor distances for other symbol pairs of the constellation.

Current standard modulation schemes are designed with equivalent nearest neighbor distances throughout the constellation, while with AsM a single nearest neighbor pair often exists. To standardize nearest neighbor distance measurements for comparisons between different constellations, average symbol energy ( $E_s$ ), or average bit energy ( $E_b$ ), needs to be used to normalize the constellations. Choice of normalization does not matter, so long as consistency is maintained, since symbol energy and bit energy are proportional to each other:

$$E_s = \log_2(M) \cdot E_b,$$

for  $M$  as the number of symbols within the constellation.

For PSK, the greatest nearest neighbor distance between symbols is achieved by evenly distributing the symbols around the unit circle, which is precisely the arrangement for symbols in standard PSK schemes. In order to alter PSK to an asymmetric design, phase difference among symbols must be altered, incidentally resulting in closer nearest neighbor pairs. Although there is a loss to signal performance in noise, an error correcting characteristic arises due to the asymmetric geometry of the constellation that mitigates the apparent cost. Further discussion will be presented in Chapter 4.

The most common QAM constellation is based on a square lattice; however if an equilateral triangle were chosen, the lattice would be more dense and result in greater normalized distances among nearest neighbor pairs. Normalized to the average energy per symbol, Figure 3.3 implies that for large constellations, the equilateral triangular lattice results in greater distances between nearest neighbor symbols.

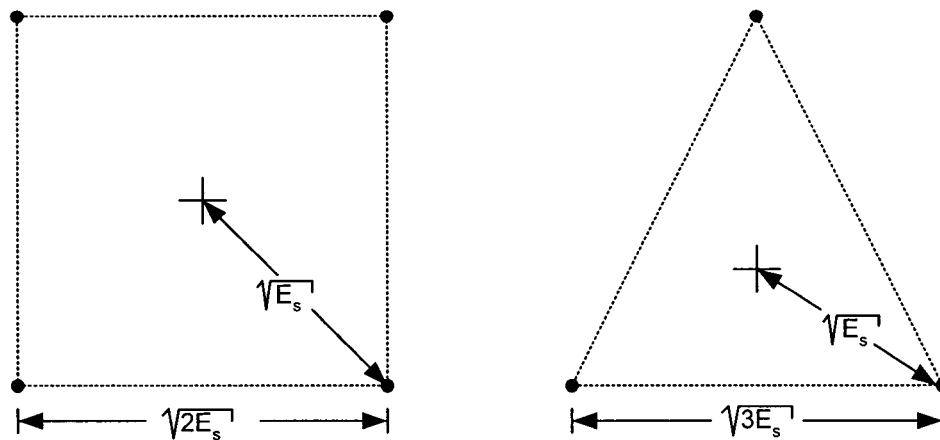


Figure 3.3 Lattice Structures

The distance (nnDist) between the nearest neighbor pair were measured with the square lattice and equilateral triangle lattice for  $M$  symbols within constellations; the results are presented in Figure 3.4: upper-left for square lattice, upper right for equilateral triangle lattice, lower half for improvement of the triangular lattice over the square lattice.

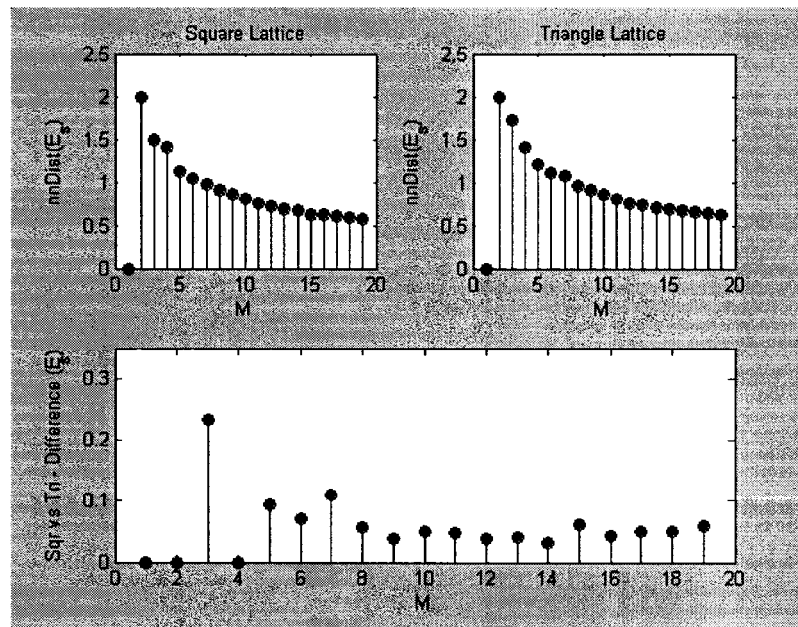


Figure 3.4 Nearest Neighbor Distance Analysis of Lattice Structures

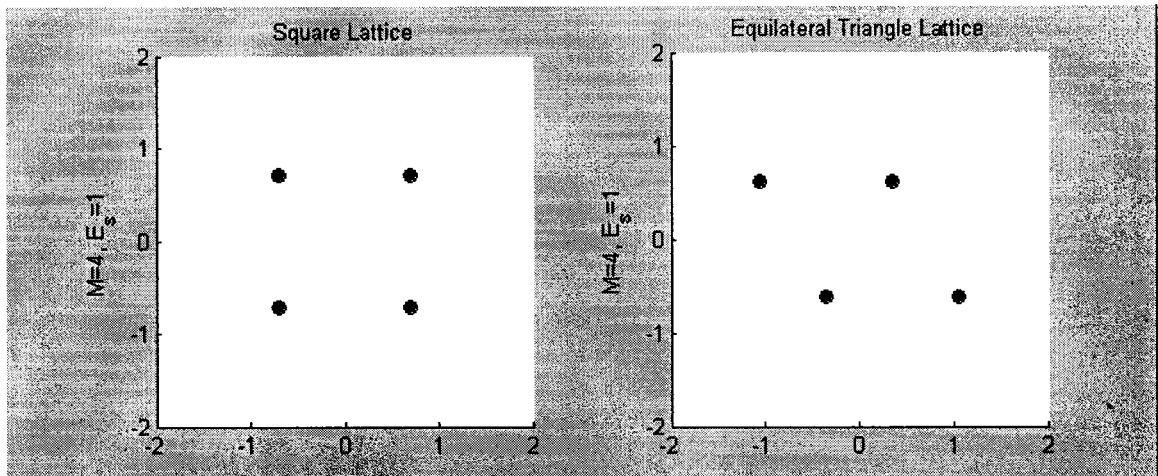


Figure 3.5 Significance of Next-to-Nearest Neighbor Intersymbol Distances

For  $M = 4$ , the nearest neighbor results were equivalent; the constellation is displayed in Figure 3.5. Note the shortest diagonal between opposite corner symbols when the triangular lattice is used. An increased potential for error over the square lattice can be deduced, since it would take less noise to cause an error between these two symbols. This demonstrates the significance of the second-to-nearest neighbor pair, and in this case the square lattice will perform better than the equilateral triangular lattice, when lattice structures are strictly adhered to. The discrepancy can be corrected by bending the lattice according to an algorithm that does not neglect the observance of symbol pairs that remain close enough to have a significant effect on performance.

### 3.4 Gray Coding

Once a constellation has been constructed to reduce symbol error, Gray coding can be applied to ensure minimal bit error. Gray coding refers to the labeling of symbols

in such a way that each symbol is uniquely labeled, with a Hamming distance of one between any given symbol and its nearest neighbor. Hamming distance refers to the number of bits that differ between two binary numbers, or symbol labels. As was alluded to earlier and will be more clearly explained in chapter 3.5, smaller distances between symbols, in AWGN systems, result in increased error potential for symbol recognition. Standard 4-QAM serves as an example and is represented in Figure 3.6, showing that the two bit hamming distance pairs can be separated by greater Euclidean distance across the diagonal, which is accomplished with Gray coding; the symbol error with two bits is less likely with Gray code.

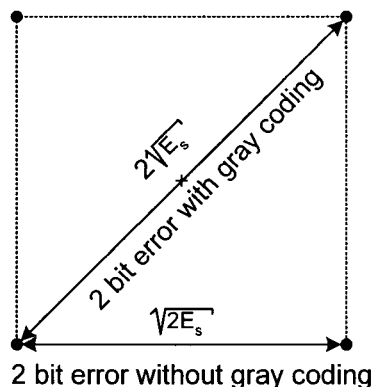


Figure 3.6 Maximizing Euclidian Distance for Large Hamming Distances

The following algorithm can be applied to symmetric PSK and slightly asymmetric AsPSK modulation schemes for Gray coding.



### PSK Gray Code Algorithm

---

S = [0 , 1]

for A = 1:log<sub>2</sub>(number\_of\_PSK\_symbols) -1

for B = 1:length(S)

S1(B) = S(B)

S2(B) = 2<sup>A</sup> + S(B)

end

S2r = reverseCellOrder(S2)

S = concatenate(S1,S2r)

end

---

S = symbol labels in order of phase

---

The benefit to AsPSK here is that more significant bits can be positioned within the constellation to have a lower probability of error than less significant bits.

Gray coding for QAM can be achieved by the following algorithm that is graphically displayed in Figure 3.7.

### Symmetric 16-QAM Gray Code Algorithm

1. establish Gray code for 4-QAM
  2. the two most significant bits of 16-QAM represent the 4-QAM Gray coded quadrants
  3. the two least significant bits of 16-QAM represent the 4-QAM Gray coded relative positions within each quadrant; however ordered clockwise or counter-clockwise relative to adjacent quadrants, so that the least significant bits are equal to the nearest neighbor symbols of the adjacent quadrant.
- 

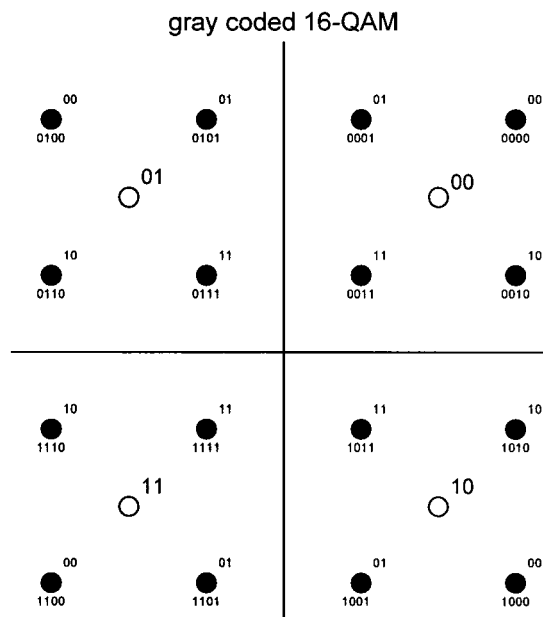


Figure 3.7 Common Gray Code for Standard 16-QAM

Other algorithms exist that may be more methodical [9] [10], but their results are equivalent, at least for standard 16-QAM, and they are still not robust enough to efficiently handle AsQAM. Decision regions in AsQAM are not as simply defined and increasing difficulties arise as denser and even randomized constellations are designed. By observing some of the characteristics of 16-QAM Gray code, an algorithm to approach AsQAM Gray coding can be developed. The resulting algorithm presented here offers an optimal approach to Gray code for asymmetric PSK or QAM constellations, and will also handle the simpler case of symmetric constellations. Some of the observations from the 16-QAM Gray code and anticipated issues for asymmetric constellations follow:

- 1) the most significant bit divides the constellation into two regions of equal symbol count,
- 2) each bit that is less significant divides the previous regions into two smaller regions, and so on until only one symbol resides in each region,
- 3) central symbols seem to have greater assurance of having a nearest neighbor hamming distance of one.

The algorithm for asymmetric Gray code, or for quasi-Gray code when Gray code is not possible, and the reason behind that approach follows:

## AsM Gray Code Algorithm

---

- 1) Initially assign all symbols to one class, since no bits have been assigned. As bits are assigned, classes are defined by the bits that have been assigned.
  - 2) Choose the two most distant symbols within any one class, and assign one as the zero seed, the other as the unity seed, chosen because they are the most likely to fall in opposite subclasses as the current classes are each being divided.
  - 3) Passively grow the decision trees from each seed, as follows:
    - a) first determine which seed is closer to another symbol, then toggle to the other seed to begin, which will be called the “passive tree” until the next toggle. Initially the passive tree only includes that seed,
    - b) identify the most distant symbol, which is not part of a current tree, to the passive tree and extend the “active tree” to include that symbol,
    - c) toggle to assign the opposite tree as passive or active, search the most distant non-tree symbol and extend the active tree to include that symbol,
    - d) continue until all symbols reside on one of the two trees,
    - e) assign the most significant available bit to ‘0’ for the zero tree and ‘1’ to the unity tree.
  - 4) Repeat step 3 with new seeds until all bits have been assigned, with the added condition that each tree can only share half of the symbols from a previously defined class
-

### 3.5 Analysis

Symbol error rates in AWGN can be approximated by doubling the number of nearest neighbor pairs in a constellation and multiplying that value times the probability of an error between a nearest neighbor pair:

$$P_e \leq \sum_{k=1}^K \operatorname{erfc}\left(\frac{d_{\min}}{2\sqrt{N_o}}\right),$$

for K as the number of nearest neighbor pairs. Probability of symbol error is a good indication of a constellation's ability to keep integrity of the information being transmitted. Probability of symbol error based on SNR will be approximated in this way for the asymmetric constellations that will be presented later.

A more valid comparison of different modulation schemes is the analysis of bit error rate (BER) versus SNR; in this document, bit energy is normalized to evaluate SNR, as  $E_b/N_o$ . The analysis used will study the effects of AWGN on asymmetric constellations and compare their performance against PSK, DPSK and QAM. As mentioned earlier, AWGN has a PDF with Gaussian distribution over the entire spectrum. In 2-PAM the theoretical analysis is straight forward; the Gaussian curve is centered over the transmitted signal with the noise variance equal to the  $N_o/2$ , such that:

$$pdf = \frac{1}{\sigma \cdot \sqrt{2 \cdot \pi}} \exp\left(\frac{-(x - \mu_x)^2}{2 \cdot \sigma^2}\right) = \frac{1}{\sqrt{\pi \cdot N_o}} \exp\left(\frac{-(x - \mu_x)^2}{N_o}\right)$$

so that integration over the region of possible error is

$$Pe = BER = \int_{\sqrt{E_b}}^{\infty} \frac{1}{\sqrt{\pi \cdot N_o}} \exp\left(-\frac{(x + \sqrt{E_b})^2}{N_o}\right) dx = \frac{1}{2} \operatorname{erfc}\left(2 \cdot \sqrt{\frac{E_b}{N_o}}\right),$$

graphically displayed in Figure 3.8.

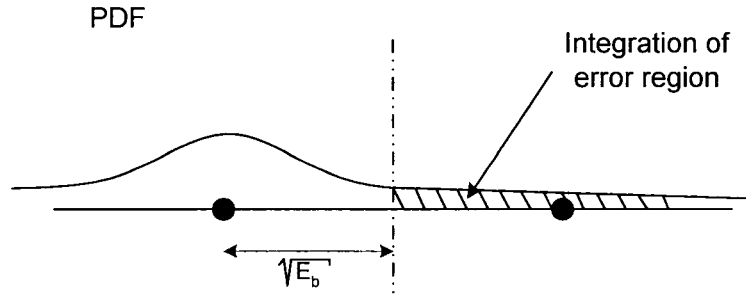


Figure 3.8 Probability of Error between Two Symbols in AWGN

Symmetric QAM and PSK can reduce the double integration to a single integration that can be solved as easily as PAM. The theoretical equations that evaluate BER against  $E_b/N_o$  for 4-PSK and 4-DPSK reduce to the well known results:

$$\text{4-PSK:} \quad BER = \frac{1}{2} \operatorname{erfc}\left(\sqrt{\frac{E_b}{N_o}}\right)$$

$$\text{4-DPSK:} \quad BER = \frac{1}{2} \exp\left(-\frac{E_b}{N_o}\right)$$

while 16-QAM is the average of possible errors among bits; assuming Gray code, the result for 16-QAM follows:

$$BER = \left[\frac{3}{4}\right] - \left[\frac{3}{8} \cdot \operatorname{erf}\left(\sqrt{\frac{2}{5}} \sqrt{\frac{E_b}{N_o}}\right)\right] - \left[\frac{1}{8} \cdot \operatorname{erf}\left(3 \cdot \sqrt{\frac{2}{5}} \sqrt{\frac{E_b}{N_o}}\right)\right] - \left[\frac{1}{8} \cdot \operatorname{erf}\left(\sqrt{\frac{6}{5}} \sqrt{\frac{E_b}{N_o}}\right)\right] - \left[\frac{1}{8} \cdot \operatorname{erf}\left(\sqrt{2} \sqrt{\frac{E_b}{N_o}}\right)\right]$$

The asymmetric constellations that we will define in the next chapter have two dimensional regions that cannot be mathematically integrated over the Gaussian PDF in closed form. The integration region for error of a single bit is represented in Figure 3.9, and polar and Cartesian coordinate equations are later presented to demonstrate that they do not have a closed form for integration.

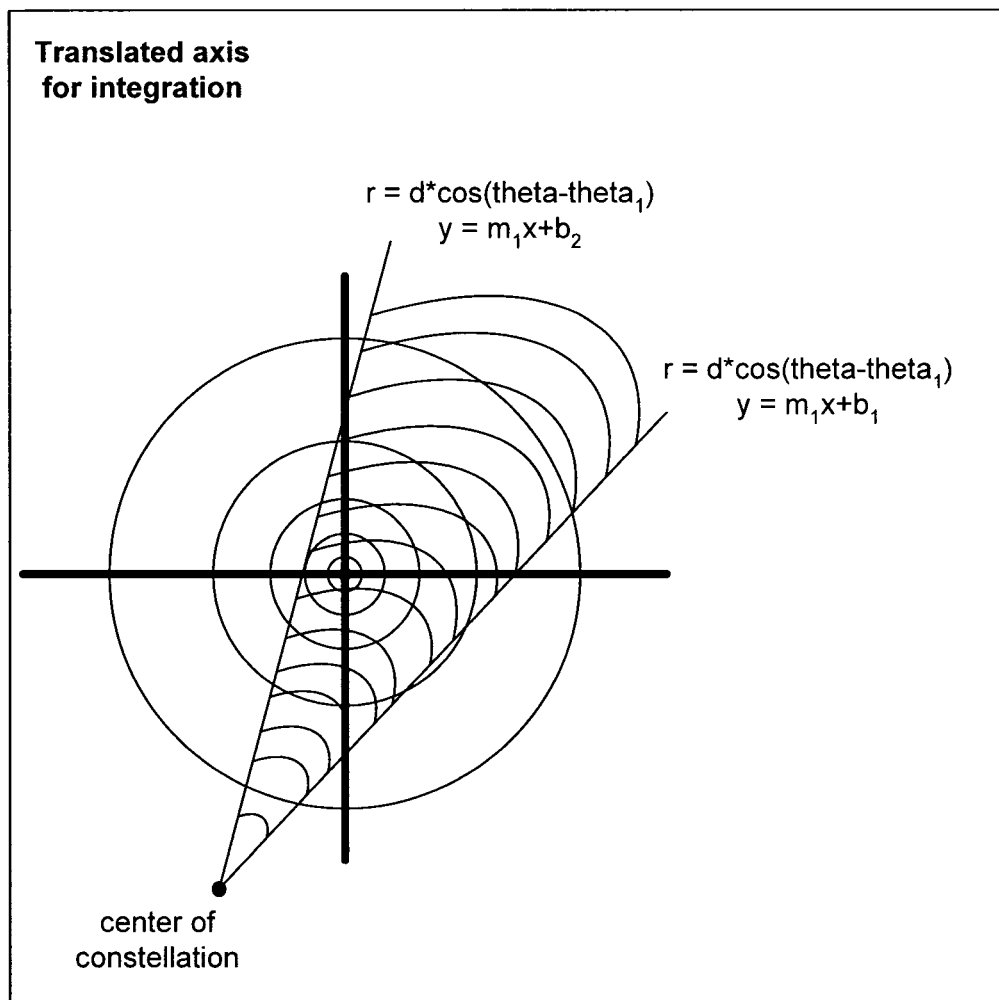


Figure 3.9 Two Dimensional Integration Region for Gaussian PDF

### Cartesian Coordinates

$$Pe = \int_A \int_{m_1x+b_1}^{m_2x+b_2} \frac{1}{2 \cdot \pi \cdot \sigma^2} \cdot e^{\left(\frac{x^2+y^2}{-2 \cdot \sigma^2}\right)} dy dx$$

$$Pe = \frac{1}{2\sqrt{2} \cdot \pi} \int_{-\frac{\pi}{2}}^{\frac{\pi}{2}} \left( e^{\left(\frac{-x^2}{2 \cdot \sigma^2}\right)} \right) \left( \operatorname{erf}\left(\frac{m_2x+b_2}{\sigma\sqrt{2}}\right) - \operatorname{erf}\left(\frac{m_1x+b_1}{\sigma\sqrt{2}}\right) \right) dx$$

*No Closed Form*

### Polar Coordinates

$$Pe = \int_{-\frac{\pi}{2}}^{\frac{\pi}{2}} \int_{d \cdot \cos(\theta+\theta_2)}^{d \cdot \cos(\theta-\theta_1)} \frac{r}{2 \cdot \pi \cdot \sigma^2} \cdot e^{\frac{-r^2}{2 \cdot \sigma^2}} dr d\theta$$

$$Pe = \frac{1}{2 \cdot \pi} \int_{-\frac{\pi}{2}}^{\frac{\pi}{2}} \left( e^{\frac{-d^2 \cdot \cos(\theta+\theta_2)^2}{2 \cdot \sigma^2}} - e^{\frac{-d^2 \cdot \cos(-\theta+\theta_1)^2}{2 \cdot \sigma^2}} \right) d\theta$$

*No Closed Form*

The solution for BER analysis will be to use the union bound on the probability of error for the asymmetric constellations. Simply stated, the union bound on the probability of error evaluates the probability of error between each pair of symbols, weights the error according to the hamming distance, and averages the results. This method proves to be a good approximation for SNRs that have BERs lower than  $10^{-3}$ . Comparison of 16-QAM's well known theoretical equation versus results of the union



bound are demonstrated in Figure 3.10 to imply the reliability of the union bound on high SNR.

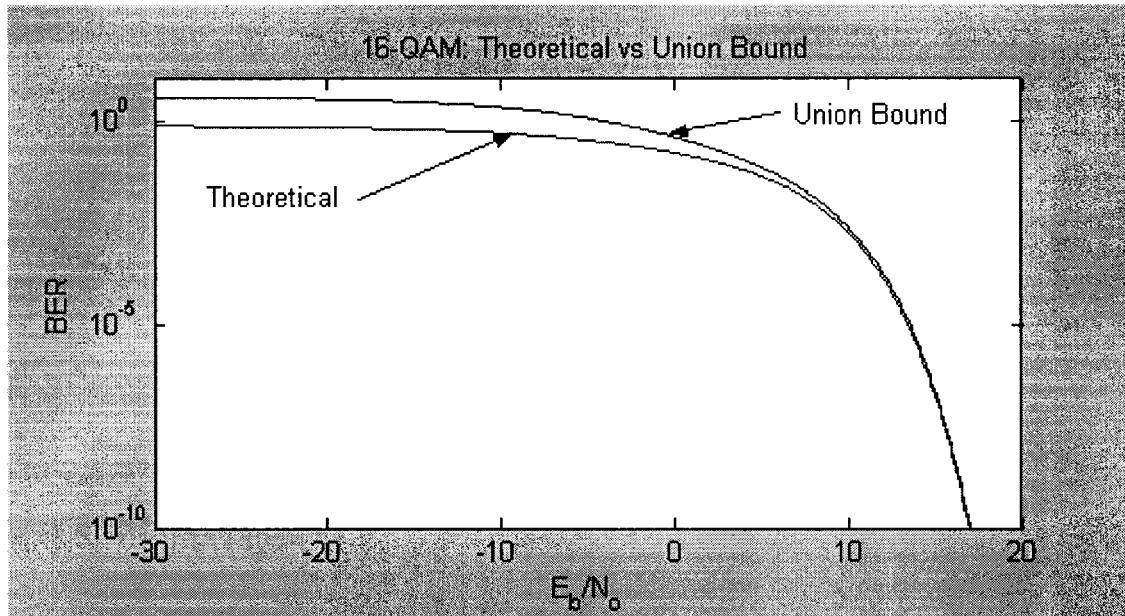


Figure 3.10 Comparison of Union Bound and Theoretical Analysis

For lower SNRs, simulations will be used to develop a more accurate graphical representation of performance in the AWGN channel, when possible. Some receivers were more complex and will need further study to present a theoretical analysis of their performance; simulation, alone, for low SNRs are presented in the stead of graphical theoretical analysis for the more advanced receiver designs.

## 4. ASYMMETRIC CONSTELLATION DESIGN

In this chapter, two versions of AsPSK and two versions of AsQAM are presented. The reasoning behind the designs and discussion on the differences of the constant and modulated signal versions are presented.

### 4.1 Early Approaches

When this project first began, the inchoate idea began simply to design phase invariant constellations, study their characteristics, and consider potential applications in communication theory. Initially, a constant amplitude design was developed to map common PSK constellations to “phase-invariant” constellations by means of an equation that applied an input variable to define a new set of phases for the symbols, to specify uniquely different constellations. Two of these initial designs are presented in chapter 4.2, as the AsPSK modulation scheme.

Next, variable amplitude constellations were designed, with a long term goal of defining a constellation in terms of peak-to-average-power ratio, or Crest factor (the ratio of peak amplitude to the rms level of the signal [11]). The first version began with PSK or QAM and mapped the amplitude according to a function that was dependent on symbol phase. Several functions were designed to map the amplitudes according to ellipses, spirals, and offset circles. The general idea is displayed in Figure 4.1, where (a) is an unaltered PAM, PSK and QAM signal; (b) is the same signals mapped with a spiral equation; and (c) is mapped with an elliptical equation.

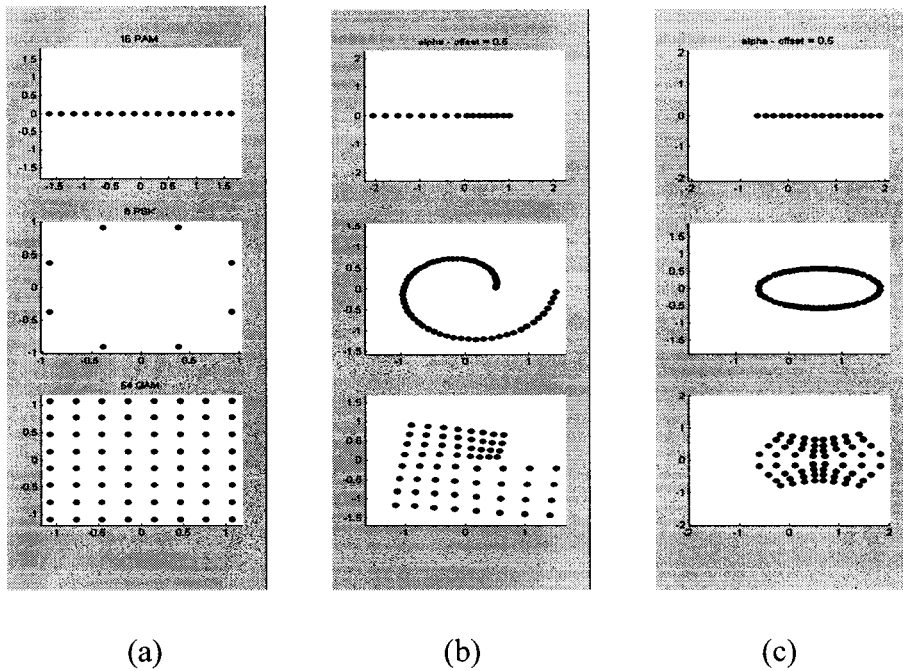


Figure 4.1 Initial Study into Phase-Invariant Modulation

A major problem was apparent, nearest neighbor distances were reduced, so an algorithm was developed to adjust phase to help maximize these distances. A further algorithm chose amplitudes according to Crest factor, and then applied a phase to maximize the nearest neighbor distances. It turned out that the densest versions didn't offer the improvement that was hoped for.

Since study of molecular lattice structures shows that denser structures can exist than structures composed of square lattices, the approach morphed to improving the lattice structure. It was found that the optimal two-dimensional lattice was constructed with equilateral triangles, and that the extension of equilateral triangles into  $N$ -dimensions was also optimal. There were drawbacks, but the difficulties were overcome and the design is presented in more detail in chapter 4.3.

## 4.2 Asymmetric Phase-Shift Keying

Asymmetric Phase-Shift Keying (AsPSK) refers to phase invariant constant envelope signals. Viewed in the complex plane, two-dimensional AsPSK constellations developed in this project are mapped from standard PSK according to equations that are dependent on a continuous design variable ranging from zero to one. The mapping functions of “AsPSK-ver1” and “AsPSK-ver2,” with “ $\alpha$ ” parameters equal to 0.3 and base constellations QPSK, are presented in Figure 4.2; their constellations are presented in Figure 4.3.

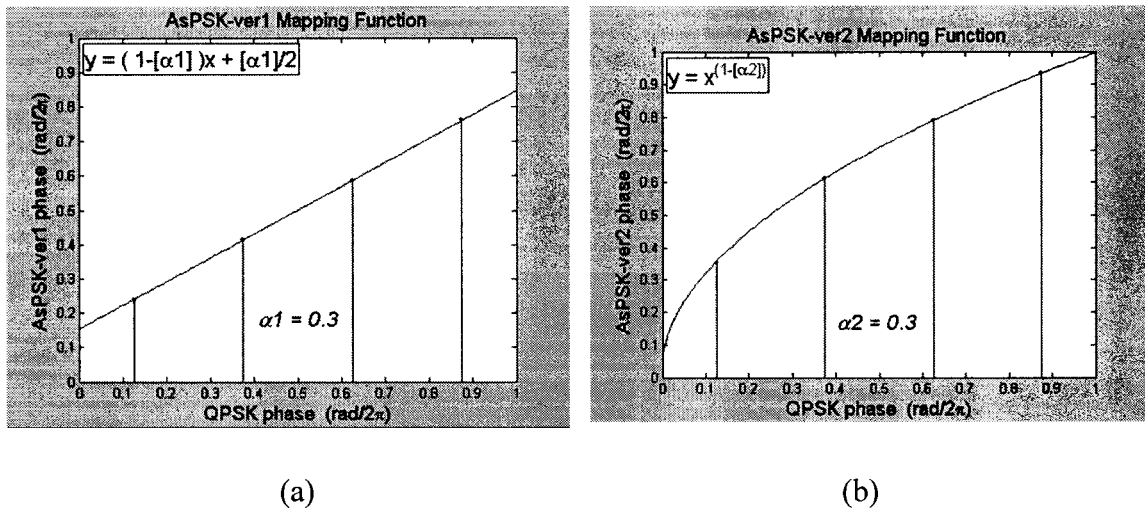


Figure 4.2 AsPSK Mapping Functions

Version-1 linearly maps phase, in order to evenly distribute the increased error among the adjacent-neighboring symbols that are drawn closer together. The result is a constellation that is phase-invariant and ambiguity-free; when all symbols are known,

phase synchronization can be established. Figure 4.4 shows multiple constellations that are available for several values of the  $\alpha_1$  parameter.

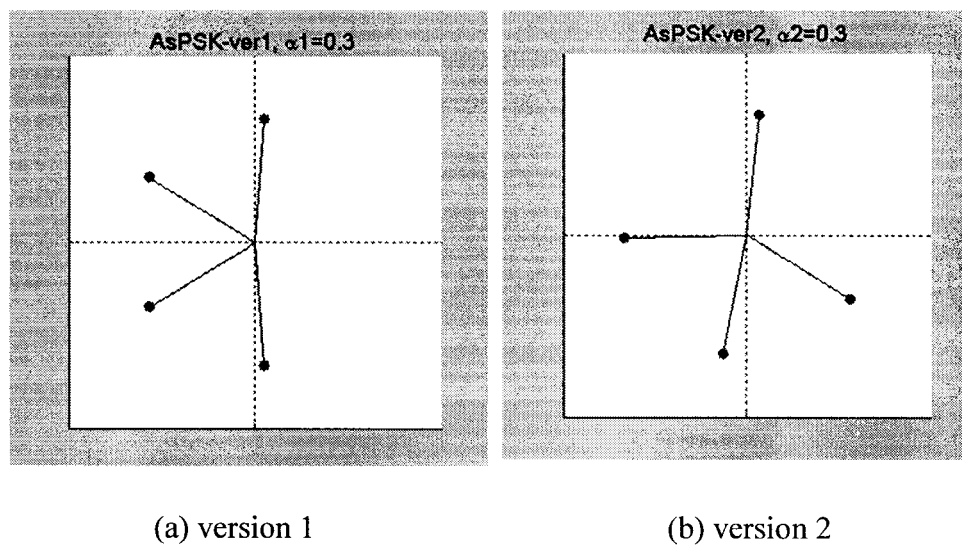


Figure 4.3 AsPSK Constellations

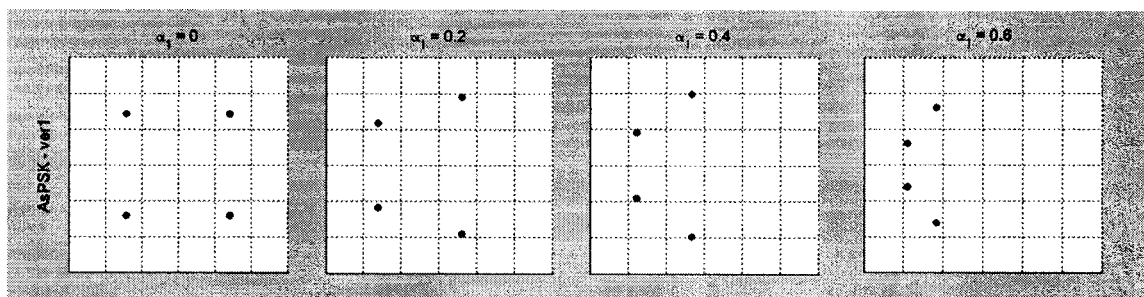


Figure 4.4 AsPSK for Various  $\alpha_1$  parameters

Version-2 uses a nonlinear mapping function to develop a fully phase-invariant, ambiguity-free constellation. The advantage over version-1 is that by knowing only two

symbols, phase synchronization can be estimated. The problem, however, is that the nearest neighboring pair is more susceptible to error than the others pairs, resulting in a constellation that is more sensitive to noise. Figure 4.5 shows multiple constellations that are available for several values of the  $\alpha_2$  parameter.

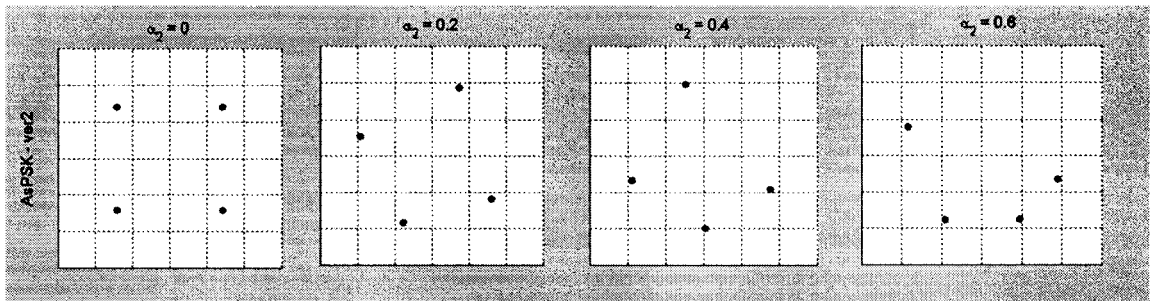


Figure 4.5 AsPSK for Various  $\alpha_2$  parameters

The probability of symbol error for AsPSK-v1 and AsPSK-v2 are derived in the following equations, where nearest neighbor distances are labeled  $d_{\min 1}$  and  $d_{\min 2}$ , SNR is  $E_s/N_0$ , probability of symbol error for the constellation in AWGN is  $P_e$ , and  $M$  is the number of symbols in the constellation.

Derivation for AsPSK-v1's upper bound for symbol probability of error in AWGN:

$$\begin{aligned}
 d_{\min\_psk} &= 2 \cdot \sqrt{E_S} \cdot \sin\left(\frac{y}{2}\right) \\
 d_{\min 1} &= 2 \cdot \sqrt{E_S} \cdot \sin\left(\frac{(1-\alpha_1)}{2} \cdot x + \frac{\alpha_1}{2}\right) \\
 d_{\min 1} &= 2 \cdot \sqrt{E_S} \cdot \sin\left(\frac{\pi}{M} + \alpha_1 \cdot \left(\frac{1}{2} - \frac{\pi}{M}\right)\right) \\
 P_e &\leq \sum_{k=1}^K \operatorname{erfc}\left(\frac{d_{\min}}{2\sqrt{N_o}}\right) \\
 P_{e1} &\leq \operatorname{erfc}\left(\frac{\sqrt{E_S}}{\sqrt{N_o}} \cdot \sin\left(\frac{\pi}{M} + \alpha_1 \cdot \left(\frac{1}{2} - \frac{\pi}{M}\right)\right)\right)
 \end{aligned}$$

Derivation for AsPSK-v2's upper bound for symbol probability of error in AWGN:

$$\begin{aligned}
 d_{\min\_psk} &= 2 \cdot \sqrt{E_S} \cdot \sin\left(\frac{y}{2}\right) \\
 d_{\min 2} &= 2 \cdot \sqrt{E_S} \cdot \sin\left(\frac{1}{2} \cdot x^{(1-\alpha_2)}\right) \\
 d_{\min 2} &= 2 \cdot \sqrt{E_S} \cdot \sin\left(\frac{1}{2} \cdot \left[ \left( \pi \left[ \frac{2 \cdot M - 1}{M} \right] \right)^{(1-\alpha_2)} - \left( \pi \left[ \frac{2 \cdot M - 3}{M} \right] \right)^{(1-\alpha_2)} \right]\right) \\
 P_e &\leq \sum_{k=1}^K \operatorname{erfc}\left(\frac{d_{\min}}{2\sqrt{N_o}}\right) \\
 P_{e2} &\leq \operatorname{erfc}\left(\frac{\sqrt{E_S}}{\sqrt{N_o}} \cdot \sin\left(\frac{1}{2} \cdot \left[ \left( \pi \left[ \frac{2 \cdot M - 1}{M} \right] \right)^{(1-\alpha_2)} - \left( \pi \left[ \frac{2 \cdot M - 3}{M} \right] \right)^{(1-\alpha_2)} \right]\right)\right)
 \end{aligned}$$

### 4.3 Asymmetric Quadrature-Amplitude Modulation

Asymmetric quadrature-amplitude modulation (AsQAM) refers to phase invariant modulated envelope signals. Two-dimensional AsQAM constellation representation

developed in this project are constructed from an equilateral triangular lattice rather than a square lattice, which is used in standard QAM designs.

$M$ -ary AsQAM-ver1 strictly adheres to the lattice structure, by adding symbols in the following order from 1 to  $M$ : symbol 1 is at the origin; symbol 2-7 are at the corners of the surrounding hexagon; symbols 8-13 are the tips of a hexagram that extends from the previous hexagon; and similar extensions to the following energy layers for additional symbols. If an energy layer is not fully occupied, there may be multiple variations of the same constellation set by selecting among the energy layer's available positions, to form unique constellations. Once the geometric structure is established, the centroid is moved to the center to minimize average energy of the constellation, and then the constellation is normalized with average symbol energy for analysis or simulation.

In the left-most graph of Figure 4.6, 16-AsQAM-ver1\_1 clearly defines the basic lattice of 13 symbols. Six potential positions in the next energy level offer four unique phase invariant arrangements for the remaining three symbols to make up the 16-symbol constellation. All variations ( $\beta_1=1,2,3,4$ ) for 16-AsQAM-ver1 are represented in Figure 4.6.

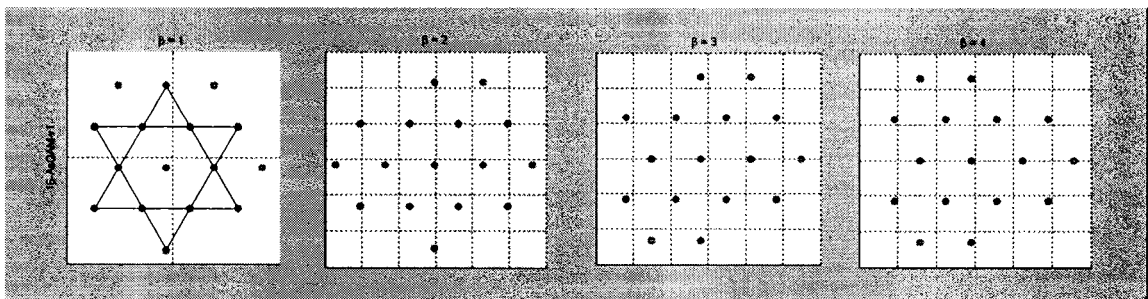


Figure 4.6 AsQAM-v1,  $\beta=[1, 2, 3, 4]$



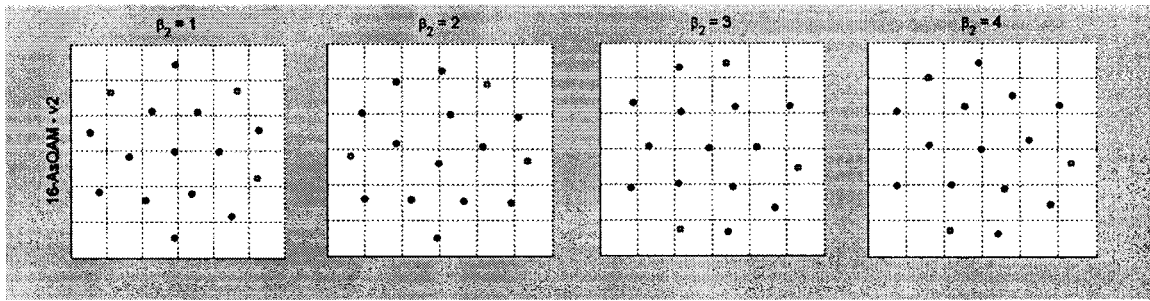


Figure 4.7 AsQAM-v2,  $\beta=[1, 2, 3, 4]$

AsQAM-ver2 takes advantage of the freedom from symmetry by bending the lattice for greater intersymbol distances and better performance when evaluated through a noisy channel. In this project we took the arrangements of version 1, and altered the positions slightly with a recursive algorithm that adjusted phase and amplitude to result in a denser, better performing algorithm. We have found that the resulting constellations are dependent on the initial lattice, so our results have four variations ( $\beta_2=1,2,3,4$ ) as with version 1. Figure 4.7 represents 16-AsQAM-ver2.

#### 4.4 Characteristics of Asymmetric Modulation

At first observation of AsPSK, it is easy to notice that these designs will have an attenuated performance for maximum likelihood (ML) detectors in noisy channels, since the nearest neighbor pairs are drawn closer together; however, there are characteristics of asymmetry that, when exploited, give rise to the potential of increased capacity, opportunity for synchronization, and functionality for noncoherent receivers.

AsQAM has a direct benefit over standard QAM, without extending observations beyond the greater distances between the nearest neighbor pairs. Applying a ML detector

immediately shows evidence of an improved signal design; moreover, the continuously controlled asymmetric characteristic of AsPSK can also be applied to AsQAM, which brings increased interest for further study of AsM.

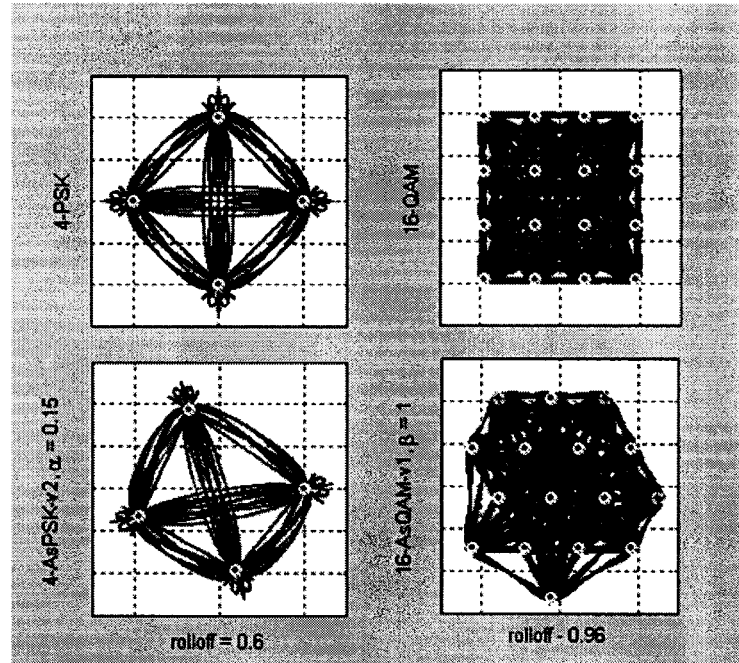


Figure 4.8 Signal Space Vector Diagrams for Symmetric and Asymmetric Signals

Eye openings for PAM signals correspond to optimum sample times; the signal space vector diagrams for PSK and QAM show the two-dimensional equivalent opportunities for clock synchronization. Figure 4.8 shows signal-space vector diagrams for AsPSK and AsQAM with rolloff factors of 0.6 and 0.96, respectively. Phase ambiguity is also removed by synchronizing signal phase in such a way as to position these eyes with consistent position in the complex plane. A circuit for employing a phase-locked loop (PLL) could be improved to correct for a wider range of phase errors

or recover the signal in a narrower band-limited channel. Also, the need for phase synchronization could even be removed, since each symbol is uniquely associated with the rest of the symbols due to the phase invariant nature of the constellation; signal detection is possible at the receiver without knowledge of the relative phase to the transmitter.

Furthermore, the asymmetry of the constellations could be shifted at the transmitter to signal frame changes without the use of additional bits in the header, or added complexity to the error correction code (ECC). For instance, AsPSK could invert the phase order of the constellation without change to its performance. Also, AsQAM could alter the Crest factor to signal frame or packet changes. This could also be used to recognize different users for different frames, or grouping IP addresses by virtue of constellation geometry. The implication: asymmetries of these types of constellations offer additional reference parameters that can be used in coding additional information into signals.

The reference parameters of asymmetry can be discrete or continuous. AsQAM-v1 was presented in the last chapter with four similar variations, discrete  $\beta$  referenced. AsPSK was presented with user defined variables, continuous  $\alpha$  referenced. Furthermore, AsQAM could be altered to either morph toward AsPSK or PSK, or stretch according to some specified function, such as those used in the early continuous approaches mentioned in chapter 4.1.

An application that these discrete and continuous reference parameters may be very useful for is software defined radio SDR and intelligent environment. If an

individual enters a room, temperature could be adjusted to best fit all occupants. A listener can express his or her likes or dislikes for a song or genre and the radio could compensate with precedence to certain occupants of the environment. All this can be transmitted with the discrete or continuous dynamic signaling mechanism of asymmetry.

The nearest neighbor pair distance for each AsQAM constellation presented are listed in Table 4.1, where the evidence of standard QAM's less efficient design is also presented in the table. The distances are normalized with the average symbol energy of the constellation. Further optimization results when version 1 is updated to version 2.

Nearest Neighbor Distances	
$\beta$	16-AsQAM-v1
1	0.6761
2	0.6688
3	0.6690
4	0.6659
16-QAM	0.6325

Table 4.1 Nearest Neighbor Distance, Normalized to Average Symbol Energy

Symbol error for AsQAM-v1 is approximated in the following equation for  $\beta=1$ :

$$P_e \leq \sum_{k=1}^K \operatorname{erfc} \left( \frac{d_{\min}}{2\sqrt{N_o}} \right) = 31 \cdot \operatorname{erfc} \left( 0.3381 \frac{\sqrt{E_s}}{\sqrt{N_o}} \right)$$

## 5. ASYMMETRIC RECEIVERS

This chapter uses MATLAB to simulate AsM signals as they pass through an AWGN channel in a complex baseband communication system model, with coherent and noncoherent receivers. Theoretical and practical analysis will evaluate BER against SNR.

The intent is to establish the potential and promise for further research with more advanced models that take into account channel characteristics such as phase estimation error and fading.

### 5.1 Coherent Receivers

For coherent receivers, it is assumed that perfect synchronization has been established between transmitter and receiver. The well known theoretical equations will be used for 4-PSK, 4-DPSK, and 16-QAM, while union bound on the probability of error will be used to estimate the performance of AsPSK and AsQAM.

For coherent AsPSK, dynamic control is implemented through an  $\alpha$  parameter that can be adjusted to compensate for channel limitations. TCP/IP protocol uses a sliding window protocol to limit the loss of dropped packets due to network anomalies; similarly when synchronizing and detecting with AsPSK, errors can be reduced by lowering the value of  $\alpha$ , while at a certain threshold, as standard PSK or  $\alpha=0$  is approached, a pilot signal could be employed to regain synchronization and signal recovery.

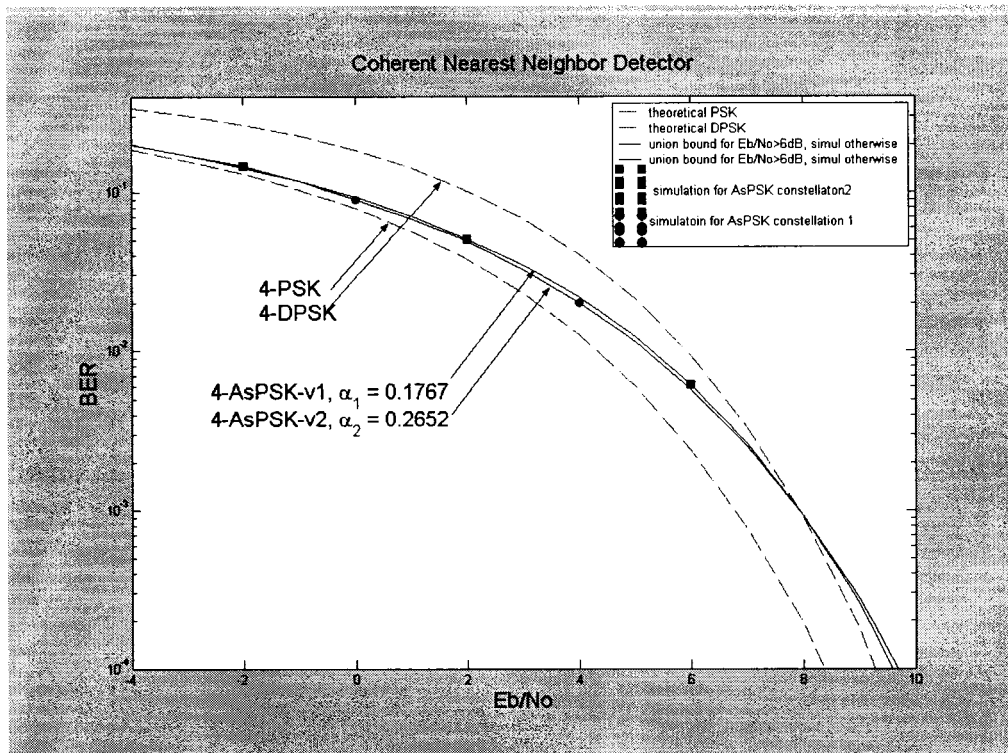


Figure 5.1 Precise Performance Control of AsPSK, against PSK & DPSK

The simulations and theoretical analysis of Figure 5.1 compare 4-AsPSK v1 & v2 to 4-PSK and 4-DPSK on the assumption that synchronization for AsPSK can be established through asymmetry. The sensitivity of the synchronization circuitry will determine how low the threshold for  $\alpha$  can be set. The known theoretical performance of DPSK was used to determine the SNR value that AsPSK has to meet to show an improvement in BER to be more useful than DPSK. Static SNR was used to evaluate the  $\alpha$  value that would result in SNR loss for maximum BERs. Figure 5.2 presents the controlled characteristic of 4-AsPSK-v2, which can be used to compensate for changes in the environment that may affect the channel and still guarantee a better performance than DPSK.

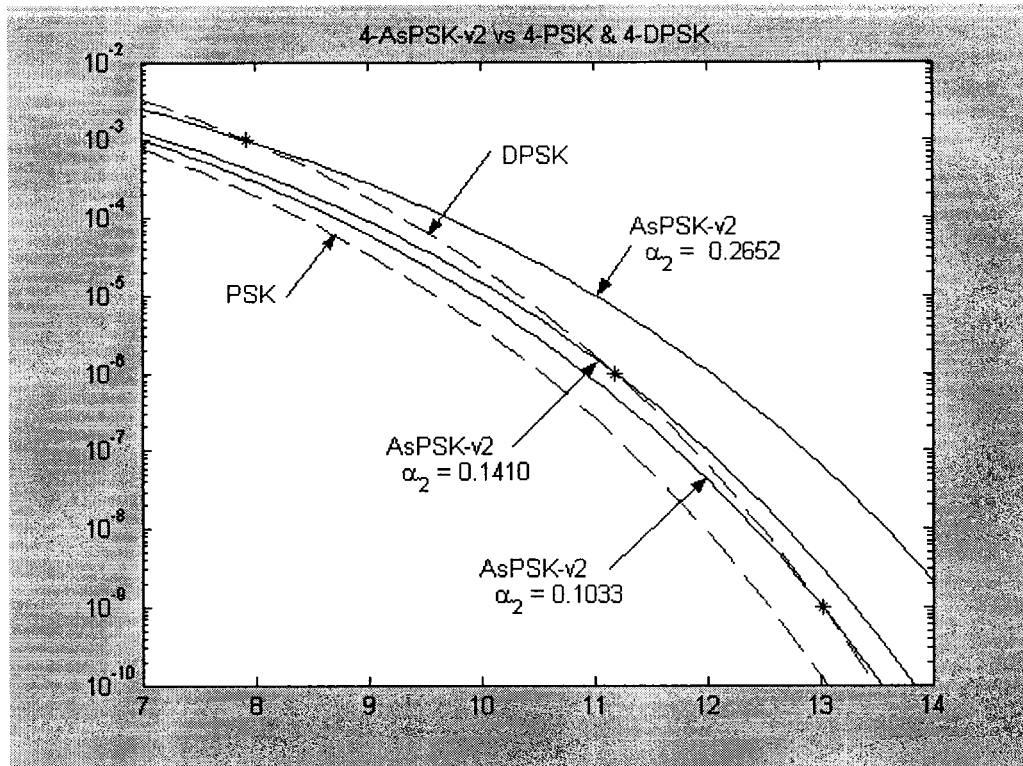


Figure 5.2 Diverse Performance Control of AsPSK, against PSK & DPSK

The analysis for AsQAM is as expected, when one takes into account the nearest neighbor pair distances that were determined in the previous chapter. 16-AsQAM-v1 with  $\beta=1$  showed a 0.5-dB SNR loss to 16-QAM for low BERs, as is presented in Figure 5.3. Similar results would result for other values of  $\beta$ .

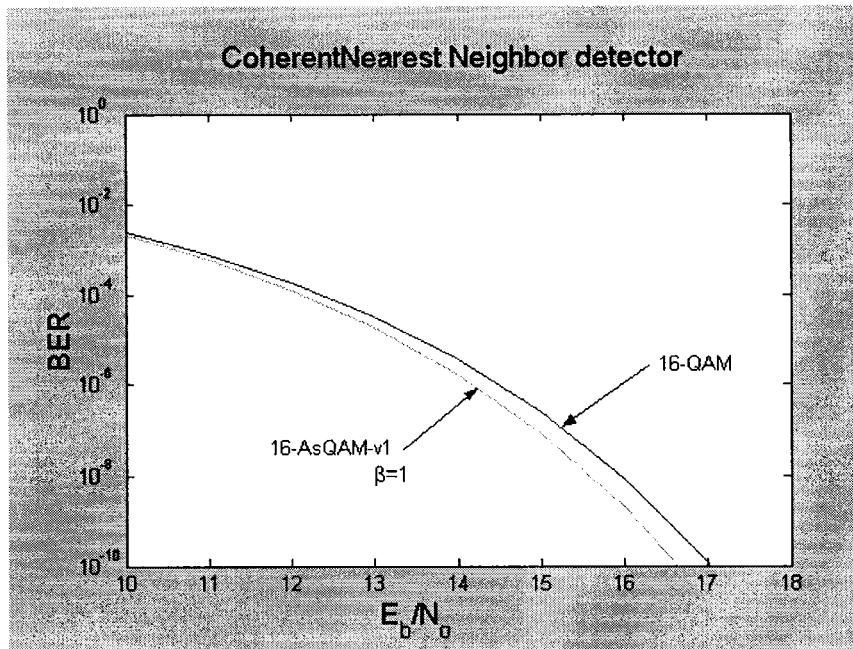


Figure 5.3 Performance Advantage of AsQAM over QAM

## 5.2 Noncoherent Receivers

Noncoherent receivers do not require knowledge of the phase for demodulation. The most common noncoherent receivers are differentially coherent receivers, which key off the previous signal vector differences to recover the original information. Asymmetrically coherent receivers, proposed in this thesis, take into account the last several signals and approximate the original signal using an analysis of the multi-cell receiving buffer. Noncoherent AsPSK has been designed and simulated, and an algorithm for implementing AsQAM along the same theory has been developed.

A block diagram of the noncoherent AsPSK receiver is presented in Figure 5.4, and the generic description of both AsPSK and AsQAM will be described in parallel, since they are very similar.



The noncoherent AsM receiver receives the signal and stores the pertinent information in the “receive-buffer” (rBuff). AsPSK stores phase only; AsQAM stores phase and amplitude of the signal vector. Relative to the oldest cell of rBuff, the positions’ relative phase, the vector is updated in the “zero-buffer” (zBuff). The “prediction-matrix” (pM) is updated on each new signal by a passive “quantization estimator” (diffQ) that is privy to the precise constellation that was sent. The prediction matrix is made up of a column for each possible symbol of the constellation, and on the assumption that the oldest cell of the rBuff is the respective prediction of each column; the other cells of each column are filled with a quantized estimate of the next signal based on the difference of the zBuff cells. The mean square difference between the prediction columns and the zBuff are calculated, and the most likely symbol is selected.

### AsPSK Hard-Decision Detector

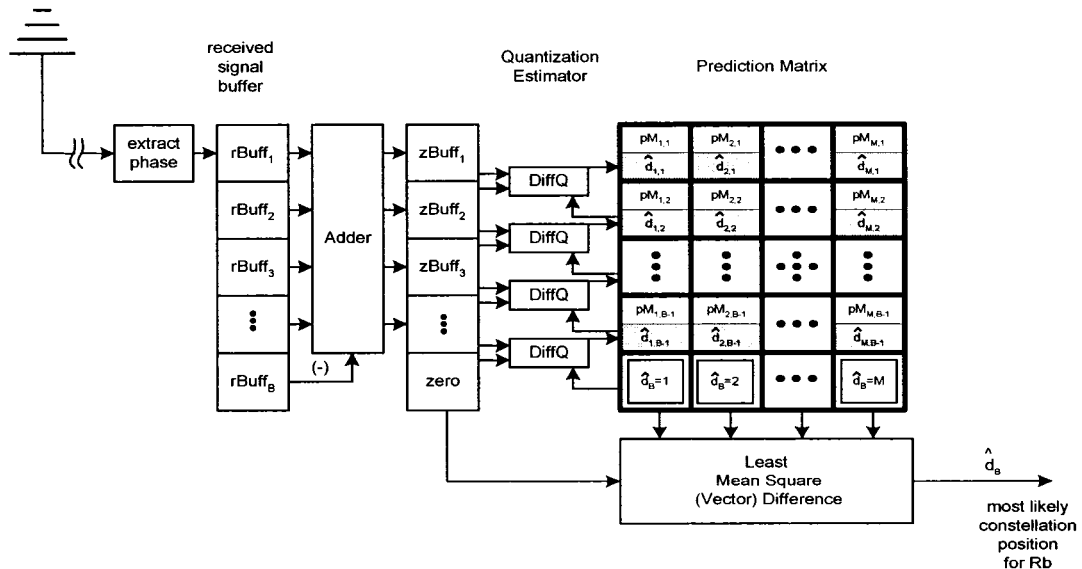


Figure 5.4 Asymmetrically Coherent Receiver

It is theorized that with an infinite buffer a certain threshold for SNR will give perfect recovery with better SNR performance than the noncoherent competition, DPSK or DQAM. Since a history is recorded, one error would be corrected; in fact, several errors would be corrected, so that an accurate estimate would be recovered. The effect would be similar to a parity check block of bits with error correction capabilities. The problem is that the computational and hardware cost may render asymmetric coherence unattainable.

The algorithm was run for 4-AsPSK-v1 and 4-AsPSK-v2 for buffer sizes of 2, 10, 50, and 200, in hopes of showing that a small buffer could effectively recover the signal from an AWGN channel. The constellations were designed with asymmetry that would perform better than DPSK up to a BER of  $10^{-3}$  with a coherent receiver described in the previous chapter. The results are presented in Figure 5.5 and 5.6.

Although we were able to establish asymmetric coherence, our results were less than anticipated. A buffer size of 200 cells would be too computationally complex to be useful, and apparently would still not successfully compete with DPSK. On the up side, another algorithm may be able to improve on this design and make use of these ideas in asymmetric modulation. Chapter 6 will present some ideas for future research on the topic of AsM, and offer different directions for future algorithms for the asymmetric receiver.

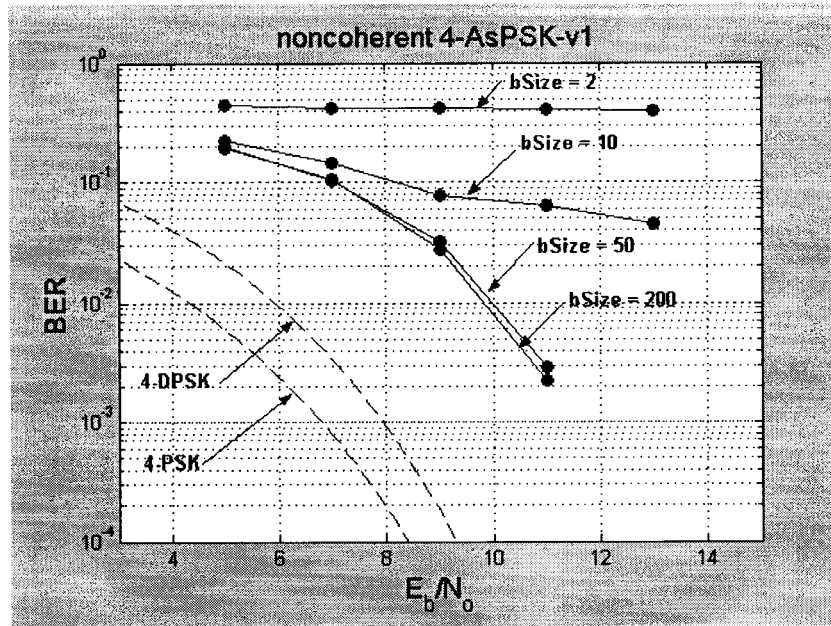


Figure 5.5 Simulation of Asymmetric Coherent Receiver with AsPSK-v1

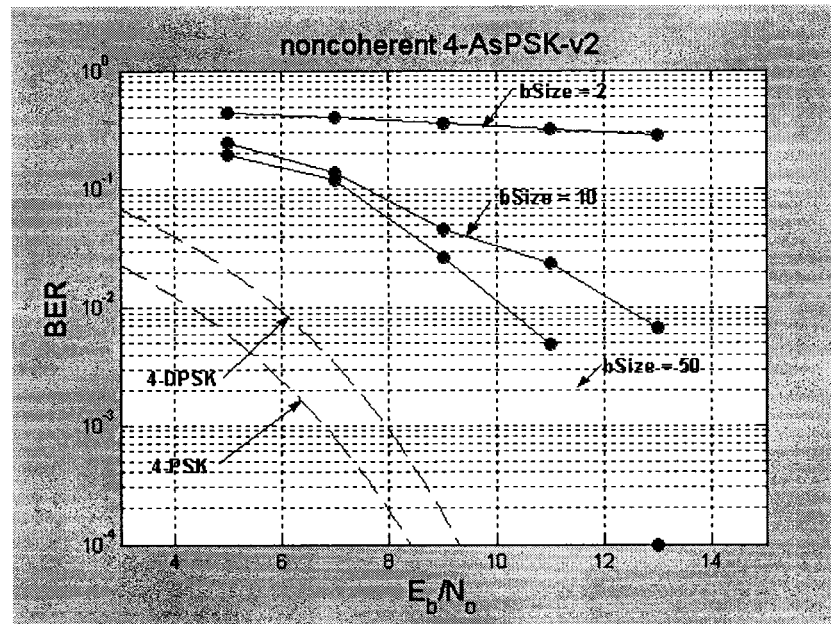


Figure 5.6 Simulation of Asymmetric Coherent Receiver with AsPSK-v2

## 6. FUTURE RESEARCH

There are many issues that should be explored to improve on the results presented in this paper. A neural network could be applied to the rBuff array. A Viterbi detector could be applied to the rBuff array. Phase synchronization could be attained through asymmetry, allowing the use of the ML algorithm presented for AsM coherent detection.

Crest factor controlled AsQAM is a viable parameter that could be used for implementing joint signal recognition. Researching the thresholds of Crest factor or AsPSK  $\beta$  differences may prove interesting topics of study.

Also, a more advanced channel model that includes phase estimation error and fading should be studied to determine the additional opportunities that AsM may offer.

Several areas for future study of AsM come to mind. This report has discussed some of the potential application for the various synchronization issues. A Gray code algorithm has been offered. AsM Receivers have been proposed that offer hope for strong breakthroughs in communication theory. The directions that this topic could take are seemingly endless at this initial stage of development.

## 7. CONCLUSION

This thesis has presented asymmetry as a reference parameter for signaling that has for the most part been overlooked by communication system theory. Not only a reference parameter, liberty from symmetric restraints also gives license to design freedoms that directly lead to better performing modulation schemes. In fact, the lattice structure we presented performs a half decibel better than standard QAM in two dimensions, and likely approaches the best possible arrangement for QAM of  $N$  dimensions. More significantly, if the asymmetric characteristic can be harnessed for carrier synchronization, the improvement over the competition, DQAM, is huge. The research in applying these new types of constellations have also lead to an algorithm for Gray coding that can apply to the trivial case of symmetric constellations, and is robust enough to be used in conjunction with the discrete and continuous asymmetry parameters that could lead to new dynamic applications for technologies such as software defined radio and intelligent environments. Moreover, synchronization issues have the potential to be resolved with lower cost, by virtue of constellation asymmetry. Similarly, Asymmetric coherence has been established, and although has yet to prove competitive to other noncoherent techniques, new algorithms that take advantage of the error correction characteristic of the constellation may soon show marked improvements over current schemes. In summary, asymmetric modulation stands a good chance of changing the way constellations are designed and implemented in complex baseband systems.

## REFERENCES

- [1] Antonio Assalini, "Improved Nyquist Pulses," *IEEE Communication Letters*, vol. 8, issue 2, page 87-89, Feb 2004
- [2] U. Mengali, A. D'Andrea, *Synchronization Techniques for Digital Receivers*, New York: Plenum Press, 1997
- [3] L. Venkata Subramaniam, Sundar Rajan, Rajendar Bahl, "Performance of 4- and 8-State TCM Schemes with Asymmetric 8-PSK in Fading Channels," *IEEE Transactions on Vehicular Technology*, vol. 49, No. 1, pg 211-219, January 2000
- [4] F. Sanzi, M. C. Necker, "Totally Blind APP Channel Estimation with Higher Order Modulation Schemes," *Proceedings of the Vehicular Technology Conference (VTC 2003-Fall)*, Orlando, October 2003
- [5] Bernard Sklar, "Rayleigh Fading Channels in Mobile Digital Communication Systems, Part I: Characterization," *IEEE Communication Magazine*, pg 90-100, July 1997
- [6] Bernard Sklar, "Rayleigh Fading Channels in Mobile Digital Communication Systems, Part II: Mitigation," *IEEE Communication Magazine*, pg 102-109, July 1997
- [7] S. Haykin, *Communication Systems*, 4th ed., New York: Wiley, 2001
- [8] J. Proakis, *Digital Communications*, Boston: McGraw Hill, 2001
- [9] Erik Agrell, Johan Lassing, Erik Strom, Tony Ottosson, "On the Optimality of the binary reflected Gray code," *IEEE Transactions on Information Theory*, 2004
- [10] Liu Wesel, "Constellation Labeling for Linear Encoders," *Conference on Information Sciences and Systems*, March 2001
- [11] Brad Anderson, "Crest Factor for Complex Signal Processing," *RF Design*, pg 40-56, October 2001